BJR https://doi.org/10.1259/bjr.20220624

Received: 21 June 2022 | Accepted: 07 February 2023 | Published online: 03 March 2023

Cite this article as:
McCabe A, Martin S, Shah J, Morgan PS, Panek R. T_1 based oxygen-enhanced MRI in tumours; a scoping review of current research. *Br J Radiol* (2023) 10.1259/bjr.20220624.

SYSTEMATIC REVIEW

T_1 based oxygen-enhanced MRI in tumours; a scoping review of current research

[1,2]ALASTAIR MCCABE, FRCR, [1]STEWART MARTIN, PhD, [3]JAGRIT SHAH, FRCR, [4,5]PAUL S MORGAN, PhD and [4,5]RAFAL PANEK, PhD

[1]Academic Unit of Translational Medical Sciences, School of Medicine, University of Nottingham, Nottingham, United Kingdom
[2]Department of Clinical Oncology, Nottingham University Hospitals NHS Trust, Nottingham, United Kingdom
[3]Department of Radiology, Nottingham University Hospitals NHS Trust, Nottingham, United Kingdom
[4]Mental Health & Clinical Neurosciences Unit, School of Medicine, University of Nottingham, Nottingham, United Kingdom
[5]Department of Medical Physics & Clinical Engineering, Nottingham University Hospitals NHS Trust, Nottingham, United Kingdom

Address correspondence to: Dr Alastair McCabe
E-mail: *alastair.mccabe@nottingham.ac.uk; alastairmccabe1@nhs.net*

Objective: Oxygen-enhanced MRI (OE-MRI) or tissue oxygen-level dependent (TOLD) MRI is an imaging technique under investigation for its ability to quantify and map oxygen distributions within tumours. The aim of this study was to identify and characterise the research into OE-MRI for characterising hypoxia in solid tumours.
Methods: A scoping review of published literature was performed on the PubMed and Web of Science databases for articles published before 27 May 2022. Studies imaging solid tumours using proton-MRI to measure oxygen-induced T_1/R_1 relaxation time/rate changes were included. Grey literature was searched from conference abstracts and active clinical trials.
Results: 49 unique records met the inclusion criteria consisting of 34 journal articles and 15 conference abstracts. The majority of articles were pre-clinical studies (31 articles) with 15 human only studies. Pre-clinical studies in a range of tumour types demonstrated consistent correlation of OE-MRI with alternative hypoxia measurements. No clear consensus on optimal acquisition technique or analysis methodology was found. No prospective, adequately powered, multicentre clinical studies relating OE-MRI hypoxia markers to patient outcomes were identified.
Conclusion: There is good pre-clinical evidence of the utility of OE-MRI in tumour hypoxia assessment; however, there are significant gaps in clinical research that need to be addressed to develop OE-MRI into a clinically applicable tumour hypoxia imaging technique.
Advances in knowledge: The evidence base of OE-MRI in tumour hypoxia assessment is presented along with a summary of the research gaps to be addressed to transform OE-MRI derived parameters into tumour hypoxia biomarkers.

INTRODUCTION

The presence of biologically significant hypoxia in tumours has been known since the work of Thomlinson and Gray in the 1950's.[1] More recent studies show that the presence of oxygen concentrations below 10 mmHg in tumours results in significantly worse radiotherapy and chemotherapy treatment outcomes as well as increasing the risk of distant metastases.[2,3] The accurate and reliable assessment of tumour hypoxia is important in identifying tumours more likely to respond to hypoxia modifying treatments and in monitoring the effect of such interventions. In addition, mapping the spatial distribution of hypoxic regions would allow targeting of treatment resistant areas with increased radiotherapy doses. Consequently, there has been significant interest in hypoxia imaging.

An emerging MRI-based technique to map hypoxia is oxygen-enhanced MRI (OE-MRI) or tissue oxygen level dependent (TOLD) MRI which only requires routinely available healthcare equipment; namely an MRI scanner and oxygen delivery mechanism. OE-MRI relies on the weakly paramagnetic property of molecular oxygen due to the presence of unpaired electrons. Elevated tissue concentrations of dissolved oxygen increase tissue's longitudinal relaxation rate ($R_1 = 1/T_1$ where T_1 is the longitudinal relaxation time).[4,5] Following the delivery of supplemental oxygen (known as an oxygen challenge), initially well-oxygenated regions where haemoglobin is well saturated develop an increase in dissolved molecular oxygen with consequential reduction in T_1 times. However in perfused hypoxic regions where haemoglobin is less well saturated, administration of high concentration oxygen leads to an

Figure 1. Example images from a patient with head and neck squamous cell carcinoma illustrating the difference between conventional T_1 weighted imaging, quantitative T_1 mapping and oxygen induced quantitative ΔT_1 maps. (A) T_1 weighted anatomical image (3D SPGR, TR/TE = 10/1.27 ms, FA = 18°). (B) Corresponding quantitative T_1 map derived using the variable flip angle methodology from image A and a corresponding proton density weighted image (not shown, acquired with same parameters but FA = 2°). (C) Oxygen induced ΔT_1 map obtained following a supplemental oxygen challenge administered using 15 L/min oxygen via a non-rebreather mask. Within the highlighted malignant nodal mass, regions of oxygen induced T_1 shortening implying normoxia are clearly seen. Distinct oxygen refractory regions are also identifiable which imply either hypoxic or non-perfused areas. FA, flip angle; TE, echo time; TR, repetition time.

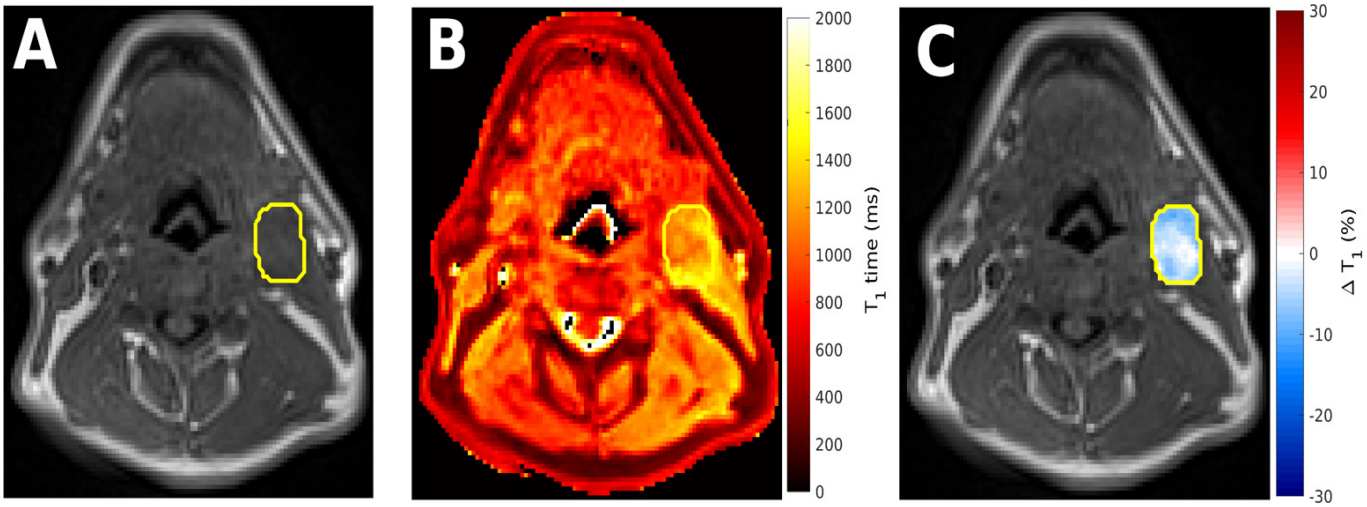

increase in oxyhaemoglobin over dissolved molecular oxygen meaning tissue T_1 times do not shorten. By administering high concentration oxygen and performing T_1 mapping, areas of hypoxia can be identified from a lack of decrease in T_1 times (Figure 1).

The purpose of this scoping review is to review the current evidence for MRI of hypoxia in solid tumours using a supplemental oxygen challenge to induce changes in proton T_1 relaxation rates and identify areas requiring further research in order to translate OE-MRI into a routinely used clinical technique.

METHODS

This scoping review follows the PRISMA extension for scoping reviews (PRISMA-ScR)[6] but was not registered on an online database. The literature search was performed on 27 May 2022 on the PubMed and Web of Science databases using identical search strategies (Appendix 1). There were no limits on publication dates.

Results from the searches were combined, duplicates removed and articles restricted to novel research. References from excluded review articles were manually examined for additional resources. Two independent reviewers screened the articles against the following inclusion criteria:

(1) Images solid tumours in animal models and/or human participants
(2) Uses proton-based MRI.
(3) Assesses changes in T_1 relaxation times (or R_1 relaxation rates, $R_1 = 1/T_1$) following a supplemental oxygen challenge

Discrepancies between reviewers were discussed and consensus reached. Grey literature was searched by interrogating abstracts from the International Society of Magnetic Resonance in Medicine annual meeting from 2011 to 2022 and the ClinicalTrials.gov website for currently open trials satisfying the eligibility criteria.

To examine the full scope of OE-MRI in solid tumours, we included pre-clinical and clinical research and did not restrict our results to a particular tumour subtype. As such, we expected significant heterogeneity in the results and relatively few publications in any one tumour type. We therefore did not plan to perform any quantitative analysis and did not have pre-defined critical appraisal criteria as we did not want to reject studies at this stage. We planned to present our findings in the form of a descriptive review.

RESULTS

227 unique records were identified. Following screening, 49 articles were identified for qualitative analysis consisting of 34 journal articles and15 conference abstracts (Figure 2, full list of results in Appendix 2). The distribution of the journal articles and published conference abstracts by publication year is shown in Figure 3. Three trials satisfying the eligibility criteria that were listed as open to recruitment were identified on the ClinicalTrials.gov website.[7–9] All of these studies have corresponding conference abstracts included in the final search results.[10–12]

Research focus

The majority of published studies involve animal only research (31 studies, 63.3%) with 15 being human only studies (30.6%) and 3 being mixed studies (6.1%). Of those involving human

Figure 2. Flowchart showing the results of the search strategy.

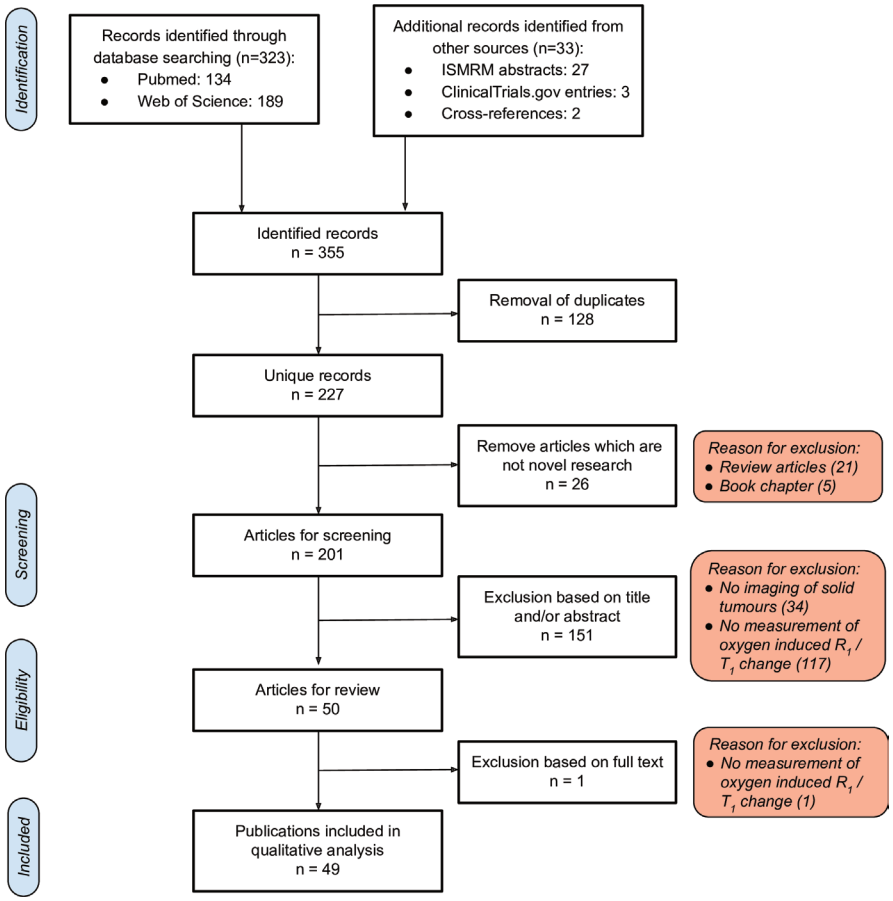

participants, 4 image intracranial neoplasms and 4 scan head and neck malignancies (22.2% each). 2 references image colorectal cancer and hepatocellular cancer (11.1% each) with the remaining results divided between single studies in lung, anal, cervical, renal, prostate and mixed tumour sites.

Pre-clinical studies

Four main associations have been tested in pre-clinical models to validate the ability of OE-MRI in detecting tumour hypoxia:

Figure 3. Histogram of publication year for journal article articles and conference abstracts identified in the search.

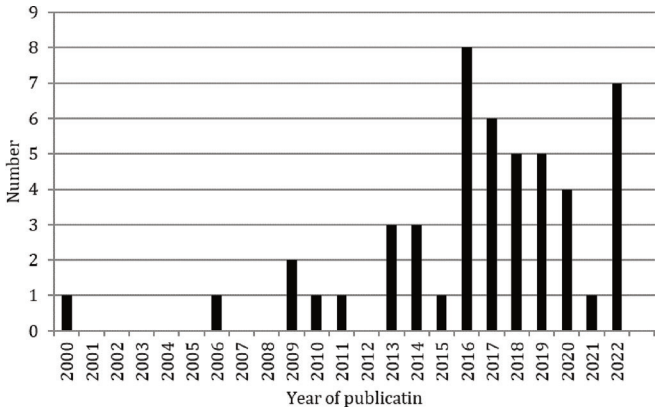

(1) Validation against alternative oxygenation determining techniques including direct measurements and alternative imaging strategies such as hypoxia PET scanning.[13–18]
(2) Verification that the distribution of hypoxic and normoxic areas seen with OE-MRI display intratumoural heterogeneity but with spatially coherent regions in keeping with patterns known to occur biologically.[5,17–35]
(3) Correlation against histopathological hypoxia indicators such as pimonidazole staining, glucose transporter 1 (GLUT-1) expression and hypoxia-inducible factor 1-α (HIF-1α) expression.[17,29,31,32,34–38]
(4) Verification of OE-MRI's ability to predict tumours more likely to display hypoxia induced treatment resistance.[16,31,39–41]

One of the papers that helped establish the utility of OE-MRI in accurately mapping tumour hypoxia was based on renal and colorectal carcinoma cell lines implanted in mice.[17] The authors correlated OE-MRI data with direct measurements of tissue oxygen concentration and established a correlation between OE-MRI quantified tumour hypoxic fraction and histopathological staining with the hypoxia sensitive marker pimonidazole. The authors also demonstrated that OE-MRI could detect expected increases in tumour hypoxic fractions following administration of the vasodilator drug hydralazine.[17] A separate study in human lung adenocarcinoma xenografts helped biologically validate the

OE-MRI technique by demonstrating its ability to detect changes in tumour hypoxic volumes following administration of a bioreductivecytotoxin (banoxantrone) and an oxygen consumption modifier (atovaquone).[40]

The original OE-MRI analysis method calculates the spatial average of T_1/R_1 changes with oxygen over the imaged tumour. However, a number of papers fail to show correlations of these spatially averaged values with reference hypoxia markers[17,24,29,42] or tumour radiosensitivity indicators[25,31,43] possibly due to the heterogeneous distributions of oxygen within tumours resulting in hypoxic regions being masked by the T_1/R_1 changes induced in normoxic areas. O'Connor et al.proposed combining OE-MRI with a perfusion assessment thereby enabling voxels of interest to be identified as perfused oxygen-enhancing (normoxia), perfused oxygen-resistant (hypoxia) or nonperfused (necrosis).[17] The perfused oxygen-resistant biomarker is sensitive to spatial fluctuations in hypoxia and shows correlation with alternative hypoxic markers and clinically relevant tumour hypoxia outcomes in both pre-clinical[17,29,31] and human studies.[29,31,44,45] Such perfusion masks have been generated using dynamic contrast-enhanced (DCE) MRI[17,29,31,44,45] and ultrasmall superparamagnetic iron oxide (USPIO)-enhanced MRI derived fractional blood volume measurements.[32]

An alternative OE-MRI approach combining R_2* (Blood Oxygen Level Dependent (BOLD)) and R_1-based oxygen-enhanced imaging aims to distinguish blood-based oxygen-induced changes from tissue-based ones. Although increased concentration of dissolved oxygen accelerates R_1 relaxation rates, the net tissue R_1 rate is affected by a number of other factors including being reduced by lower concentrations of deoxyhaemoglobin.[46] Although this influence is generally small compared to the influence of dissolved oxygen, the simultaneous measurement of R_2* values may yield insights into the cause of observed oxygen-induced tissue R_1 decreases.[20,25,36,47,48] In particular, Cao-Pham et al present a hypothesis based on their work on rhabdomyosarcoma and glioma xenografts where they divide voxels into four classes dependent upon the relative changes in oxygen induced R_1 and R_2* rates[25]:

(1) *Normoxia:* Significantly increasing R_1 (increased molecular oxygen) and stable or mildly increased R_2* (stable deoxy/oxyhaemoglobin ratio)
(2) *Mild hypoxia:* Slightly increasing R_1 (increased molecular oxygen) with decreasing R_2* (decreased deoxy/oxyhaemoglobin ratio). Assumes unsaturated baseline haemoglobin changing to near complete saturation.
(3) *Severe hypoxia*: No/mild decreasing R_1 and decreasing R_2* (decreased deoxy/oxyhaemoglobin ratio)
(4) *Vascular Steal:* Decreasing R_1 with increasing R_2*. Hypothesised to be caused by dilatation of mature blood vessels shunting blood away from tumour regions served by immature vessels resulting in decreased blood volume and molecular oxygen.

The use of a cyclical oxygen challenge combined with independent component analysis of the voxel-wise signal traces has been proposed as another method to improve the sensitivity of OE-MRI. Hypoxic regions derived using this approach have been correlated to pimonidazole stained areas in murine squamous cell carcinomas[38] and shown capable of detecting oxygenation changes in murine tumours following treatment with vascular growth factor inhibition.[30] However, poor correlation with human colorectal xenografts was noted possibly due to the lack of a perfusion assessment meaning that regions of necrosis may have confounded the imaging assessment.[38]

Regarding correlations of OE-MRI parameters with preclinical treatment outcomes, 3 studies in prostate cancer found oxygen-induced R_1 changes correlated with outcomes following radiotherapy[16,39,41] but 1 paper found no association between OE-MRI parameters and local tumour control probability.[43] This study used tumour mean oxygen-induced R_1 changes rather than the perfused fraction biomarker. Salem et al found that OE-MRI determined biomarkers detected therapy-induced changes in hypoxia in glioma xenografts and non-small cell lung cancer (NSCLC)[31] but all studies that have looked at correlating OE-MRI biomarkers with treatment outcomes have been with relatively small study sizes.

Table 1. Summary of principle research focus of tumour OE-MRI studies in humans categorised by domains derived from the CRUK and EORTC consensus statement on the clinical translation of imaging biomarkers[49]

Clinical research focus	Number of studies	References
Proof of principle including safety, feasibility and tolerability	15	5,10–12,21,31,36,44,45,50–55
Repeatability and reproducibility	5	31,44,50,54,55
Correlation with histopathology	2	29,56
Changes of biomarkers with treatment	7	11,31,45,52,53,55,57
Initial correlation of biomarkers to clinical outcomes	1	52
Prospective, adequately powered studies linking biomarkers to clinical outcomes	0	N/A
Analysis techniques	7	5,21,28,29,31,36,58
Multicentre studies	0	N/A
Health economic considerations	0	N/A

CRUK, Cancer Research UK; EORTC, European Organisation for Research and Treatment of Cancer.

Human studies

OE-MRI studies on human participants have been performed on all major anatomical regions with no significant difficulties reported with patient tolerability. The principle research foci of the human studies are shown in Table 1 categorised by domains derived from the Cancer Research UK and European Organisation for Research and Treatment of Cancer consensus statement on the clinical translation of imaging biomarkers.[49]

Three studies performed OE-MRI assessments in both preclinical and clinical settings and all demonstrate similar patterns between animal and human scans.[29,31,36] The studies investigating changes of OE-MRI biomarkers with treatment in patients have been performed in glioblastoma, [57] brain metastases,[53] head

and neck cancer,[55] NSCLC,[31] cervical cancer,[11] rectal cancer[45] and anal cancer.[52]

Salem et al used the perfused hypoxic fraction metric in patients with NSCLC to distinguish tumours that have persistent hypoxia from those that demonstrate hypoxia modification with chemoradiotherapy.[31] Similarly, Little et al scanned patients with rectal cancer immediately prior to chemoradiotherapy and again at day 7 or day 14 of treatment and found measurable changes in tumour hypoxic burden with treatment using the perfused Oxy-R metric. Reduction in tumour hypoxia was only apparent by day 14 though and not at day 7.[45] Reduction in hypoxic fractions with treatment is also found in the anal, cervical and head and neck cancer studies with the latter additionally demonstrating the feasibility of performing OE-MRI on the MR-Linac (hybrid MRI scanner and radiotherapy linear accelerator).[11,52,55]

Technical considerations

A range of methodologies have been used in clinical OE-MRI research (Tables 2 and 3). Human studies show a preference for 1.5 T (11 studies, 61.1%) over 3 T (9 studies, 50.0%) imaging systems (2 studies utilised both field strengths). The most frequently used T_1 measurement technique in human OE-MRI is the variable flip angle (VFA) method, used by 50% of studies, closely followed by inversion recovery-based techniques. An alternative T_1 mapping technique called MOBILE (mapping of oxygen by imaging lipids relaxation enhancement) that exploits the increased solubility of oxygen in lipids over water has also been investigated.[14] Studies in tumour models found that oxygen induced changes in lipid R_1 rates were of greater magnitude than changes in water R_1 and global R_1rates.[14,15] This approach however might be sensitive to the amount of lipid present within tumours.[42]

OE-MRI can be performed statically with T_1 mapping performed before and after oxygen or dynamically during the switch from air to oxygen (Tables 2 and 3). The duration of hyperoxia delivered before repeat imaging in human studies ranges from 2 to 15 min. For the 6 human studies that provide a dynamic scan duration, the median OE-MRI acquisition time was 22.5 min (range 7–32 min).

Oxygen delivery

The oxygen challenge was delivered in the form of 100% oxygen in 35 studies (71.4%) and carbogen (mixture of oxygen and carbon dioxide) in 9 studies (18.4%) with 2 studies using both and 3 unstated. In the human studies, the majority use 100% oxygen (15 studies, 83.3%) with 2 using carbogen (11.1%) and 1 using both. Carbogen has been investigated as an alternative to 100% oxygen with the aim of mitigating the vasoconstrictive effect of hyperoxia with the vasodilative influence of carbon dioxide.[15,16,19,20,22,23,25,33] However, Winter et al found that varying the carbon dioxide concentration in administered carbogen had no significant effect on altering blood flow during OE-MRI[19] and Hallac *et al* found similar OE-MRI responses in prostate cancer xenografts with carbogen and 100% oxygen.[16] It should be noted that in animal experiments,high concentration oxygen is also a crucial component of the anaesthetic process, therefore potentially affecting baseline oxygenation levels compared to awake animals.

The use of an internal quality control point to provide a quantitative assessment of adequate oxygen delivery has been proposed because inadequate oxygen delivery during an OE-MRI scan could result in inappropriate labelling of regions as oxygen challenge refractory. Such control regions have been located in skeletal muscle,[5] renal cortices,[29] descending thoracic aorta,[31], uterine body[11] and nasal conchae.[55]

DISCUSSION

Overall, there is strong pre-clinical evidence that OE-MRI can accurately and reliably detect hypoxic regions of solid tumours and monitor how such regions change with anticancer therapies. The evidence base for OE-MRI from clinical studies is, however, much less advanced. Initial results from human trials are promising for the utility of OE-MRI in tumour hypoxia imaging, however, due to the early stage nature of this research all of these studies are single institute trials without prospective power calculations and without standardised data acquisition or analysis methodologies. Further work is required on specific tumour sites in patients to optimise and standardise OE-MRI protocols as well as establish the optimum timing to correlate OE-MRI data to clinically relevant outcomes before validating OE-MRI biomarkers in larger multicentre trials.

Currently, there is no consensus on the optimal imaging sequence to use in OE-MRI. Given the heterogeneous nature of oxygenation within tumours, it is unsurprising that most researchers have opted for three-dimensional acquisitions in order to map the entire tumour volume. Indeed those clinical studies that opted for single slice acquisitions have struggled with co-registering images acquired during treatment with baseline data.[10,52] The accuracy and precision of T_1 determination is not equivalent between different methodologies though; VFA, *e.g.* consistently overestimates T_1 values in the brain.[59,60] However, as it is the change in T_1 times that is relevant in OE-MRI, this may mitigate somewhat systematic errors in T_1 measurement. Work to develop a consensus guideline, such as exists in DCE MRI,[61] balancing the competing demands of acquisition time, spatial coverage, temporal resolution and measurement accuracy is critical in standardising tumour OE-MRI imaging and allowing for comparison of studies.

If OE-MRI were to be added to routine clinical diagnostic protocols, the duration of the OE-MRI sequence is critical with respect to health resources, patient tolerability and the risk of movement and image quality degradation. The extent and nature of movement during OE-MRI scans will vary depending upon the anatomical area of interest; however, it is clear that appropriate image co-registration techniques are required for robust data analysis.[10,12,31] Currently, there is a large range in the duration of clinical OE-MRI scans and variations between dynamic imaging and static acquisitions. The optimal duration of the oxygen challenge in patients is not yet proven and the potential benefits of delivering multiple oxygen challenges during one imaging session thus facilitating independent component data analysis

Table 2. Imaging parameters and setup details for the T_1-based oxygen-enhanced MR scans for the peer-review published in human studies

	O'Connor et al. 2009[5]	Remmele et al. 2013[21]	Linnik et al. 2014[36]	Bane et al. 2016[49]	Hectors et al. 2017 a[55]	Hectors et al. 2017 b[55]	Zhou, Hallac. et al. 2017[50]	Little et al. 2018[29]	Salem et al. 2019[31]	Bluemke et al. 2020[51]	Qian et al. 2020[52]	Bluemke et al. 2022 a[10]	Bluemke et al. 2022 b[10]
Area	Liver, omentum, pelvis	Brain	Brain	Liver	Liver	Liver	Prostate	Kidney	Lung	Anus	Brain	Head and neck	Head and neck
B0	1.5T	3T	3T	1.5T	3T	1.5T (3T)	3T	1.5T	1.5T	3T	3T	3T	3T
Sequence	3D FFE	2D-SPGR simultaneous R1/R2*	3D FFE	IR-LL	3D VFA	2D IR-LL	FFE	IR	IR-prepared3D-SPGR	MOLLI	FFE	MOLLI	IR-prepared3D-SPGR
TR / TE (ms)	3.5/0.9	103/12 echoes	3.5/1.1	2.26/1.04	10/1.2	2.3/1.0 (35.1/1.2)	-	10,000/3.1	2.1/0.5	3,000/120	32/2.0	3.05/1.332	4/0.656
TI (ms)	-	-	-	42–1576.5	-	42-1577 (80–1445)	-	50, 200, 500, 10000, 20000, 5000, 1400 (dynamic)	10, 50, 300, 1100 (dynamic), 2000, 5000	11 inversion times	-	11 inversion times	-
Flip angles (°)	2, 8, 17	25	2, 5, 10, 16	8	1, 10, 19	8 (10)	2 to 14 (5 angles)	45	6	35	7, 16, 37	35	2, 5, 10, 15
No. slices	25	40	25	1-2	36	1-2	-	1	41	1	-	1	-
Slice (mm)	4	5	4.2	8	5	8	3	7	5	5	5	10	5
FoV (mm)	375	230	230	420 × 288.75	350 × 260	420 × 290 (320 × 280)	240 to 260	375	450	380	240	-	-
Resolution (mm)	2.93	1.8	1.8	3.3	0.9	3.3 (1.0)	0.94	2.93	4.69	1.7	1.88	-	-
Dynamic / Static	Dynamic	Dynamic	Dynamic	Static	Static	Static	Static	Dynamic	Dynamic	Static	Static	Static	Static
Temp res. (s)	20	2.3	68	-	-	-	-	30	10	-	-	-	-
Hyperoxia	100% (15L/min)	Carbogen: 95% O_2	100% (15L/min)	100 % / Carbogen	15 L/min for 10–15 mins	15 L/min for 10–15 mins	100% for 7 mins	100% (15L/min)	100% (15L/min)	100% until end tidal O2 = 70%	100% for 3 min	100% until end tidal O_2 = 70%	100% until end tidal O_2 = 70%
Oxygen delivery device	Non-rebreathing circuit with Hudson mask.	Mask	Non-rebreathing mask	Non-rebreathing mask	-	-	Face mask	Non-rebreathing mask	Non-rebreathing Hudson mask via gas blender	Non-rebreathing mask	Non-rebreathing mask	Non-rebreathing mask	Non-rebreathing mask
Coils	Body	Head	Head	Spine and body	Spine and body	Spine and body	Cardiac and endorectal	Body	Body	Body	Head	Head	Head
Duration baseline	24 readings	1 min	11 readings	1 reading	1 reading	1 reading	1 reading	9 readings	12/18 readings	1 reading	1 reading	1 reading	1 reading
Duration oxygen	48 readings	4 min	12 readings	1 reading	1 reading	1 reading	1 reading	-	48 readings	1 reading	1 reading	1 reading	1 reading
OE-MRI duration	32 mins	7 min	26 min	20 s per reading	14 s per image	18 s (10 s) per image	-	-	26 mins	-	-	-	-

FFE, Fast Field Echo; IR, Inversion Recovery; IR-LL, Inversion Recovery Look-Locker; MOLLI, Modified Look-Locker Inversion Recovery; SPGR, Spoiled gradient recalled acquisition in the steady state;VFA, Variable Flip Angle.

Table 3. Imaging parameters and setup details for the T_1 based oxygen-enhanced MR scans for the conference abstracts of human studies

	Panek et al. 2018[44]	Little et al. 2019[45]	Datta et al. 2022[11]	Dubec et al. 2022[54]	McCabe et al. 2022[12]	Prezzi et al. 2022 a[53]	Prezzi et al. 2022 b[53]
Area	Head and neck	Rectum	Cervix	Head and neck	Head and neck	Rectum	Rectum
B_0	3T	1.5T	1.5T	1.5T	1.5T	3T	3T
Sequence	3D SPGR	3D SPGR	IR prepared 3D SPGR	IR prepared 3D SPGR	Dixon	3D SPGR	MOLLI
TR / TE (ms)	4.5/2.3	12/0.74	2.2/0.66	2.8 to 3.0/0.9 to 1.0	7.3/2.39 & 4.77 ms	4.56/2.04	280.56/1.12
TI (ms)	-	-	100, 500, 1100 (dynamic), 2000, 4300	100, 500, 800, 1100 (dynamic), 4300	-	-	180
Flip angles (°)	3, 16	3, 13, 18	4	6	2, 12	2, 13	35
No. slices	24	25	-	-	72	72	1
Slice (mm)	2.5	4	6	5	2.5	3	8
FoV (mm)	240	375	384	384	200	380 × 309	360 × 307
Resolution (mm)	1.5	2.34	3	3	1.6	1.2	1.4
Dynamic / Static	Dynamic	Dynamic	Dynamic	Dynamic	Static	Static	Static
Temp res. (s)	3	13.9	12	12	-	-	-
Hyperoxia	100%	100%	100%	100%	100% for ≥ 7 mins	100% for ≥ 3 mins	100% for ≥ 3 mins
Oxygen delivery device	Non-rebreathing mask	Non-rebreathing mask	Non-rebreathing mask	Non-rebreathing mask	Non-rebreathing mask	-	-
Coils	Head and neck	-	-	-	Posterior head / anterior flex	-	-
Duration baseline	20 readings	14 readings	25 readings	25 readings	5 readings	6 readings	6 readings
Duration oxygen	210 readings	-	45 readings	45 readings	5 readings	6 readings	6 readings
OE-MRI duration	-	-	19 mins	19 mins	8.6 s per reading	40 s per reading	8.5 s per reading

IR, Inversion Recovery; MOLLI, Modified Look-Locker Inversion Recovery;SPGR, Spoiled gradient recalled acquisition in the steady state.
No imaging parameters were provided for one abstract.[56]

techniques has not been proven to outweigh the difficulties of increased scan time.

With regards to the delivery of the oxygen challenge, although there are legitimate concerns regarding the vasoconstrictive effects of hyperoxia confounding the OE-MRI signal, the evidence presented suggests that in practice this is not a significant issue. In addition, inhalation of carbogen gas has been shown to induce unpredictable responses in different organs[62] as well as not always being well tolerated in humans due to its potential to cause dyspnoea. It therefore seems reasonable for future human studies to use 100% oxygen rather than carbogen, however, the risk of hyperoxic vasoconstriction should be considered. In addition, future studies should continue to use quality control points to provide quantitative evidence of adequate tissue oxygen delivery. The location of such points will depend on the anatomical area imaged, the field of view used and the imaging sequence. Standardisation of such markers will be helpful for future multicentre trials.

Novel methods of OE-MRI data analysis continue to be developed and offer the potential to increase the accuracy of OE-MRI in differentiating regions of tumour hypoxia. Although the use of the perfused hypoxic fraction metric has been successfully applied in clinical OE-MRI studies, it does require a co-registered perfusion assessment which may limit its clinical utility. Alternative approaches such as synchronous BOLD and OE-MRI measurements, independent or principle component data

analysis and novel data clustering techniques may ultimately prove to be more effective hypoxia categorisation tools. Further work is required to correlate data clustering approaches to clinically relevant outcomes and to optimise OE-MRI data processing approaches.

The optimal timing of when to perform OE-MRI assessments of tumours in patients undergoing treatment is not yet clear. Baseline metrics of hypoxic fraction may provide a stratification methodology for the utilisation of novel hypoxia activated drugs or novel radiosensitisers in patients more likely to respond to them but the more sensitive application of OE-MRI biomarkers may be in identifying regional hypoxia that is invariant to treatment. The initial patient studies looking at such repeat scans in OE-MRI show that the timing of the reassessments is crucial but this may also be dependent on tumour type and therapy modality and requires further evaluation. In addition, the clinical implication of chronic tumour hypoxia *vs* transient or cycling hypoxia and the potential for OE-MRI to distinguish between these has not been fully explored as yet. Dynamic or repeated oxygen challenge imaging may allow rapid frequency cycling tumour hypoxia characteristics to be elucidated with OE-MRI, whereas repeat assessment on different days is more likely to reveal changes in chronic hypoxia levels.[63] Separating out these two components of hypoxia may provide a more powerful OE-MRI metric and requires further research.

There are some limitations with this scoping review. Firstly, due to the relatively novel nature of OE-MRI in solid tumours just over 30% of the published articles identified are conference abstracts rather than journal articles. These abstracts have not been through the same level of peer review that journal articles are subject to; however, we felt that it was important to include this grey literature in order to present the full scope of research being performed in this area. Secondly, our inclusion criteria explicitly states that we are interested in studies that quantify oxygen induced T_1 or R_1 changes, however, this means at least three studies that assessed changes in T_1 weighted signal intensity were excluded from the analysis.[64–66] Finally, we did not search all available medical or scientific databases but focussed on two that we felt were most likely to yield the greatest number of results. Future reviews may benefit from using alternative databases in order to obtain the most comprehensive search results.

In conclusion, there is strong pre-clinical evidence of the utility of OE-MRI in assessing and monitoring tumour hypoxia, however, significant clinical work remains to be completed before OE-MRI-derived biomarkers can be utilised as a routine component of cancer imaging.

ACKNOWLEDGEMENTS

The authors have received a research grant from Nottingham University Hospitals Charity (APP2361/N0379). PSM is a member of the UK National Institute of Health Research's Nottingham Biomedical Research Centre.

CONFLICT OF INTEREST

The authors have no conflicts of interest to disclose.

REFERENCES

1. THOMLINSON RH, GRAY LH. The histological structure of some human lung cancers and the possible implications for radiotherapy. *Br J Cancer* 1955; **9**: 539–49. https://doi.org/10.1038/bjc.1955.55
2. Dewhirst MW, Cao Y, Moeller B. Cycling hypoxia and free radicals regulate angiogenesis and radiotherapy response. *Nat Rev Cancer* 2008; **8**: 425–37. https://doi.org/10.1038/nrc2397
3. Hughes VS, Wiggins JM, Siemann DW. Tumor oxygenation and cancer therapy-then and now. *Br J Radiol* 2019; **92**(1093): 20170955. https://doi.org/10.1259/bjr.20170955
4. Tadamura E, Hatabu H, Li W, Prasad PV, Edelman RR. Effect of oxygen inhalation on relaxation times in various tissues. *J Magn Reson Imaging* 1997; **7**: 220–25. https://doi.org/10.1002/jmri.1880070134
5. O'Connor JPB, Naish JH, Parker GJM, Waterton JC, Watson Y, Jayson GC, et al. Preliminary study of oxygen-enhanced longitudinal relaxation in MRI: a potential novel biomarker of oxygenation changes in solid tumors. *International Journal of Radiation Oncology*Biology*Physics* 2009; **75**: 1209–15. https://doi.org/10.1016/j.ijrobp.2008.12.040
6. Tricco AC, Lillie E, Zarin W, O'Brien KK, Colquhoun H, Levac D, et al. PRISMA extension for scoping reviews (PRISMA-scr): checklist and explanation. *Ann Intern Med* 2018; **169**: 467–73. https://doi.org/10.7326/M18-0850
7. Choudhury A. MR-BIO: A study to evaluate changes in MR imaging and biological parameters - full text view - clinicaltrials.gov. Internet. clinicaltrials.gov. 2021. Available from: https://clinicaltrials.gov/ct2/show/NCT04903236
8. Datta A. Biomarkers for clinical hypoxia evaluation in cervical cancer. Internet. ClinicalTrialsGov. 2021. Available from: https://clinicaltrials.gov/ct2/show/NCT05029258
9. Panek R, McCabe A. Evaluation of OE-MRI in patients with head and neck cancer. [Internet]. *ClinicalTrialsGov* 2021. Available from: https://clinicaltrials.gov/ct2/show/NCT04724096
10. Bluemke E, Bertrand A, Chu K-Y, Syed N, Murchison AG, Cooke R, et al. Using variable FLIP angle (VFA) and modified look-locker inversion recovery (MOLLI) T1 mapping in clinical OE-MRI. *Magn Reson Imaging* 2022; **89**: 92–99. https://doi.org/10.1016/j.mri.2022.03.001
11. Datta A, Dubec M, Buckley D, McHugh D, Salah A, Little R, et al. Quantifying and mapping hypoxia modification in patients with uterine cervical cancer using oxygen-enhanced MRI. *Proc Intl Soc Mag Reson Med* 2022; 2584.
12. McCabe A, Christian J, Panek R. Oxygen-induced MRI T1 changes in head and neck anatomical structures. *Clinical Radiology* 2022; **77**: e1–2. https://doi.org/10.1016/j.crad.2022.09.003
13. Pacheco-Torres J, Zhao D, Saha D, Lopez-Larrubia P, Cerdan S, Mason RP. Evaluation of lung tumor oxygenation using FREDOM and TOLD. *Proc Intl Soc Mag Reson Med* 2009; 2464.
14. Jordan BF, Magat J, Colliez F, Ozel E, Fruytier A-C, Marchand V, et al. Mapping of oxygen

by imaging lipids relaxation enhancement: a potential sensitive endogenous MRI contrast to map variations in tissue oxygenation. *Magn Reson Med* 2013; **70**: 732–44. https://doi.org/10.1002/mrm.24511
15. Colliez F, Neveu MA, Magat J, Cao Pham TT, Gallez B, Jordan BF. Qualification of a noninvasive magnetic resonance imaging biomarker to assess tumor oxygenation. *Clin Cancer Res* 2014; **20**: 5403–11. https://doi.org/10.1158/1078-0432.CCR-13-3434
16. Hallac RR, Zhou H, Pidikiti R, Song K, Stojadinovic S, Zhao D, et al. Correlations of noninvasive BOLD and told MRI with PO2 and relevance to tumor radiation response. *Magn Reson Med* 2014; **71**: 1863–73. https://doi.org/10.1002/mrm.24846
17. O'Connor JPB, Boult JKR, Jamin Y, Babur M, Finegan KG, Williams KJ, et al. Oxygen-enhanced MRI accurately identifies, quantifies, and maps tumor hypoxia in preclinical cancer models. *Cancer Res* 2016; **76**: 787–95. https://doi.org/10.1158/0008-5472.CAN-15-2062
18. Zhou H, Chiguru S, Hallac RR, Yang D, Hao G, Peschke P, et al. Examining correlations of oxygen sensitive MRI (BOLD/TOLD) with [^{18}f]FMISO PET in rat prostate tumors. *Am J Nucl Med Mol Imaging* 2019; **9**: 156–67.
19. Winter JD, Akens MK, Cheng HLM. Quantitative MRI assessment of VX2 tumour oxygenation changes in response to hyperoxia and hypercapnia. *Phys Med Biol* 2011; **56**: 1225–42. https://doi.org/10.1088/0031-9155/56/5/001
20. Burrell JS, Walker-Samuel S, Baker LCJ, Boult JKR, Jamin Y, Halliday J, et al. Exploring δR (2) * and δR (1) as imaging biomarkers of tumor oxygenation. *J Magn Reson Imaging* 2013; **38**: 429–34. https://doi.org/10.1002/jmri.23987
21. Remmele S, Sprinkart AM, Müller A, Träber F, von Lehe M, Gieseke J, et al. Dynamic and simultaneous Mr measurement of R1 and R2* changes during respiratory challenges for the assessment of blood and tissue oxygenation. *Magn Reson Med* 2013; **70**: 136–46. https://doi.org/10.1002/mrm.24458
22. Zhao D, Pacheco-Torres J, Hallac RR, White D, Peschke P, Cerdán S, et al. Dynamic oxygen challenge evaluated by NMR T1 and T2* -- insights into tumor oxygenation. *NMR Biomed* 2015; **28**: 937–47. https://doi.org/10.1002/nbm.3325
23. Beeman SC, Shui YB, Perez-Torres CJ, Engelbach JA, Ackerman JJH, Garbow JR. O 2 -sensitive MRI distinguishes brain tumor versus radiation necrosis in murine models. *Magn Reson Med* 2016; **75**. https://doi.org/10.1002/mrm.26276
24. Rich LJ, Seshadri M. Photoacoustic monitoring of tumor and normal tissue response to radiation. *Sci Rep* 2016; **6**: 21237. https://doi.org/10.1038/srep21237
25. Cao-Pham T-T, Joudiou N, Van Hul M, Bouzin C, Cani PD, Gallez B, et al. Combined endogenous mr biomarkers to predict basal tumor oxygenation and response to hyperoxic challenge. *NMR Biomed* 2017; **30**(12). https://doi.org/10.1002/nbm.3836
26. Zhou H, Belzile O, Zhang Z, Saha D, Wagner J, Sishc B, et al. Evaluation of tumor oxygenation following radiation and PS-targeting antibody therapy in an orthotopic lung cancer model. *Proc Intl Soc Mag Reson Med* 2017; 4364.
27. Zhou H, Zhang Z, Denney R, Williams JS, Gerberich J, Stojadinovic S, et al. Tumor physiological changes during hypofractionated stereotactic body radiation therapy assessed using multi-parametric magnetic resonance imaging. *Oncotarget* 2017; **8**: 37464–77. https://doi.org/10.18632/oncotarget.16395
28. Featherstone AK, O'Connor JPB, Little RA, Watson Y, Cheung S, Babur M, et al. Data-Driven mapping of hypoxia-related tumor heterogeneity using DCE-MRI and OE-MRI. *Magn Reson Med* 2018; **79**: 2236–45. https://doi.org/10.1002/mrm.26860
29. Little RA, Jamin Y, Boult JKR, Naish JH, Watson Y, Cheung S, et al. Mapping hypoxia in renal carcinoma with oxygen-enhanced MRI: comparison with intrinsic susceptibility MRI and pathology. *Radiology* 2018; **288**: 739–47. https://doi.org/10.1148/radiol.2018171531
30. Moosvi F, Baker JHE, Yung A, Kozlowski P, Minchinton AI, Reinsberg SA. Dynamic Oxygen-Enhanced MRI (dOE-MRI) with group ICA detects increased oxygenation in murine tumours treated with VEGF-ablation therapy. Proc Intl Soc Mag Reson Med. 2019;27.
31. Salem A, Little RA, Latif A, Featherstone AK, Babur M, Peset I, et al. Oxygen-enhanced MRI is feasible, repeatable, and detects radiotherapy-induced change in hypoxia in xenograft models and in patients with non-small cell lung cancer. *Clin Cancer Res* 2019; **25**: 3818–29. https://doi.org/10.1158/1078-0432.CCR-18-3932
32. Lepicard E, Boult J, Jamin Y, Zormpas-Petridis K, Featherstone A, Box C, et al. Imaging hypoxia in head and neck cancer xenografts with oxygen-enhanced MRI. *Proc Intl Soc Mag Reson Med* 2020; 0276.
33. Waschkies CF, Pfiffner FK, Heuberger DM, Schneider MA, Tian Y, Wolint P, et al. Tumor grafts grown on the chicken chorioallantoic membrane are distinctively characterized by MRI under functional gas challenge. *Sci Rep* 2020; **10**(1): 7505. https://doi.org/10.1038/s41598-020-64290-z
34. Boult JKR, Roy U, Bernauer C, Box C, Howell L, Lepicard EY, et al. Characterising hypoxia in rhabdomyosarcoma xenografts with oxygen-enhanced MRI. *Proc Intl Soc Mag Reson Med* 2022; 2754.
35. Roy U, Lepicard EY, Boult JKR, Box C, Harrington KJ, O'Connor JPB, et al. Imaging hypoxia in murine oral cavity squamous cell carcinomas with oxygen-enhanced MRI. *Proc Intl Soc Mag Reson Med* 2022; 0289.
36. Linnik IV, Scott MLJ, Holliday KF, Woodhouse N, Waterton JC, O'Connor JPB, et al. Noninvasive tumor hypoxia measurement using magnetic resonance imaging in murine U87 glioma xenografts and in patients with glioblastoma. *Magn Reson Med* 2014; **71**: 1854–62. https://doi.org/10.1002/mrm.24826
37. Li X, Qin S, Liang W, Mei Y, Yuan Y, Quan X. Assessment of tumor hypoxia using tissue oxygen level dependent in a rabbit VX2 liver tumor model. *Proc Intl Soc Mag Reson Med* 2018.
38. Moosvi F, Baker JHE, Yung A, Kozlowski P, Minchinton AI, Reinsberg SA. Fast and sensitive dynamic oxygen-enhanced MRI with a cycling gas challenge and independent component analysis. *Magn Reson Med* 2019; **81**: 2514–25. https://doi.org/10.1002/mrm.27584
39. White DA, Zhang Z, Li L, Gerberich J, Stojadinovic S, Peschke P, et al. Developing oxygen-enhanced magnetic resonance imaging as a prognostic biomarker of radiation response. *Cancer Lett* 2016; **380**: 69–77. https://doi.org/10.1016/j.canlet.2016.06.003
40. Little RA, Tessyman V, Babur M, Cheung S, Watson Y, Gieling R, et al. In vivo OE-MRI quantification and mapping of response to hypoxia modifying drugs banoxantrone and atovaquone in calu6 xenografts. *Proc Intl Soc Mag Reson Med* 2017; 2919.
41. Arai TJ, Yang DM, Campbell JW III, Chiu T, Cheng X, Stojadinovic S, et al. Oxygen-Sensitive MRI: a predictive imaging biomarker for tumor radiation response? *International Journal of Radiation Oncology*Biology*Physics* 2021; **110**: 1519–29. https://doi.org/10.1016/j.ijrobp.2021.03.039
42. Cao-Pham T-T, Tran L-B-A, Colliez F, Joudiou N, El Bachiri S, Grégoire V, et al. Monitoring tumor response to carbogen breathing by oxygen-sensitive magnetic resonance parameters to predict the outcome of radiation therapy: a preclinical

study. *International Journal of Radiation Oncology*Biology*Physics* 2016; **96**: 149–60. https://doi.org/10.1016/j.ijrobp.2016.04.029
43. Belfatto A, White DA, Mason RP, Zhang Z, Stojadinovic S, Baroni G, et al. Tumor radio-sensitivity assessment by means of volume data and magnetic resonance indices measured on prostate tumor bearing rats. *Med Phys* 2016; **43**: 1275–84. https://doi.org/10.1118/1.4941746
44. Panek R, Wong KH, Welsh L, Riddell AM, Koh DM, Morgan V, et al. Oxygen-enhanced MRI for the detection of hypoxia in patients with head and neck cancer. *Proc Intl Soc Mag Reson Med* 2018; 3916.
45. Little RA, Datta A, Featherstone AK, Watson Y, Cheung S, Buckley L. DCE-MRI and DWI provide complementary response evaluation in patients with rectal cancer treated with chemoradiotherapy. *Proc Intl Soc Mag Reson Med* 2019.
46. Bluemke E, Stride E, Bulte DP. A general model to calculate the spin-lattice relaxation rate (R1) of blood, accounting for hematocrit, oxygen saturation, oxygen partial pressure, and magnetic field strength under hyperoxic conditions. *J Magn Reson Imaging* 2022; **55**: 1428–39. https://doi.org/10.1002/jmri.27938
47. Yang DM, Arai TJ, Campbell JW 3rd, Gerberich JL, Zhou H, Mason RP. Oxygen-Sensitive MRI assessment of tumor response to hypoxic gas breathing challenge. *NMR Biomed* 2019; **32**(7): e4101. https://doi.org/10.1002/nbm.4101
48. O'Connor JPB, Robinson SP, Waterton JC. Imaging tumour hypoxia with oxygen-enhanced MRI and BOLD MRI. *Br J Radiol* 2019; **92**(1095): 20180642. https://doi.org/10.1259/bjr.20180642
49. Bane O, Besa C, Wagner M, Oesingmann N, Zhu H, Fiel MI, et al. Feasibility and reproducibility of bold and told measurements in the liver with oxygen and carbogen gas challenge in healthy volunteers and patients with hepatocellular carcinoma. *J Magn Reson Imaging* 2016; **43**: 866–76. https://doi.org/10.1002/jmri.25051
50. Zhou H, Hallac RR, Yuan Q, Ding Y, Zhang Z, Xie X-J, et al. Incorporating oxygen-enhanced MRI into multi-parametric assessment of human prostate cancer. *Diagnostics (Basel)* 2017; **7**(3): 48. https://doi.org/10.3390/diagnostics7030048
51. Bluemke E, Bulte D, Bertrand A, George B, Cooke R, Chu K-Y, et al. Oxygen-enhanced MRI MOLLI T1 mapping during chemoradiotherapy in anal squamous cell carcinoma. *Clinical and Translational Radiation Oncology* 2020; **22**: 44–49. https://doi.org/10.1016/j.ctro.2020.03.001
52. Qian J, Yu X, Li B, Fei Z, Huang X, Luo P, et al. In vivo monitoring of oxygen levels in human brain tumor between fractionated radiotherapy using oxygen-enhanced MR imaging. *CMIR* 2020; **16**: 427–32. https://doi.org/10.2174/1573405614666180925144814
53. Prezzi D, Neji R, Dregely I, Jeljeli S, Bassett P, Cook G, et al. Feasibility and repeatability of oxygen-enhanced T1 measurements in primary colorectal cancer: a prospective study in 22 patients. *Proc Intl Soc Mag Reson Med* 2022; 3421.
54. Dubec M, Datta A, Little RA, Clough A, Buckley DL, Hague C, et al. First in-human technique translation of OE-MRI for hypoxia imaging onto an MR linac system in patients with head and neck cancer. *Proc Intl Soc Mag Reson Med* 2022.
55. Hectors SJ, Wagner M, Bane O, Besa C, Lewis S, Remark R, et al. Quantification of hepatocellular carcinoma heterogeneity with multiparametric magnetic resonance imaging. *Sci Rep* 2017; **7**(1): 2452. https://doi.org/10.1038/s41598-017-02706-z
56. Zhou H, Wilson D, Lickliter J, Ruben J, Raghunand N, Sellenger M, et al. TOLD MRI validation of reversal of tumor hypoxia in glioblastoma with a novel oxygen therapeutic. *Proc Intl Soc Mag Reson Med* 2016; 3576.
57. Little RA, Parker GJM, O'Connor JPB. Quantifying confidence in the OE-MRI biomarker pOxy-R using bootstrap analysis. Proc Intl Soc Mag Reson Med. 2022;30.
58. O'Connor JPB, Aboagye EO, Adams JE, Aerts HJWL, Barrington SF, Beer AJ, et al. Imaging biomarker roadmap for cancer studies. *Nat Rev Clin Oncol* 2017; **14**: 169–86. https://doi.org/10.1038/nrclinonc.2016.162
59. Stikov N, Boudreau M, Levesque IR, Tardif CL, Barral JK, Pike GB. On the accuracy of T1 mapping: searching for common ground. *Magn Reson Med* 2015; **73**: 514–22. https://doi.org/10.1002/mrm.25135
60. Taylor AJ, Salerno M, Dharmakumar R, Jerosch-Herold M. T1 mapping: basic techniques and clinical applications. *JACC Cardiovasc Imaging* 2016; **9**: 67–81. https://doi.org/10.1016/j.jcmg.2015.11.005
61. Shukla-Dave A, Obuchowski NA, Chenevert TL, Jambawalikar S, Schwartz LH, Malyarenko D, et al. Quantitative imaging biomarkers alliance (QIBA) recommendations for improved precision of DWI and DCE-MRI derived biomarkers in multicenter oncology trials. *J Magn Reson Imaging* 2019; **49**: e101–21. https://doi.org/10.1002/jmri.26518
62. O'Connor JPB, Jackson A, Buonaccorsi GA, Buckley DL, Roberts C, Watson Y, et al. Organ-Specific effects of oxygen and carbogen gas inhalation on tissue longitudinal relaxation times. *Magn Reson Med* 2007; **58**: 490–96. https://doi.org/10.1002/mrm.21357
63. Bader SB, Dewhirst MW, Hammond EM. Cyclic hypoxia: an update on its characteristics, methods to measure it and biological implications in cancer. *Cancers (Basel)* 2020; **13**(1): 23. https://doi.org/10.3390/cancers13010023
64. Fan Q, Tang CY, Gu D, Zhu J, Li G, Wu Y, et al. Investigation of hypoxia conditions using oxygen-enhanced magnetic resonance imaging measurements in glioma models. *Oncotarget* 2017; **8**: 31864–75. https://doi.org/10.18632/oncotarget.16256
65. Lloyd WK, Agushi E, Coope D, Lewis D, Jackson A, Parker GJM. An optimised protocol for dynamic oxygen enhanced imaging of brain tumours. Proc Intl Soc Mag Reson Med. 2019;27.
66. Liu H, Zheng L, Shi G, Xu Q, Wang Q, Zhu H, et al. Pulmonary functional imaging for lung adenocarcinoma: combined MRI assessment based on IVIM-DWI and OE-UTE-MRI. *Front Oncol* 2021; **11**: 677942. https://doi.org/10.3389/fonc.2021.677942
67. Kinoshita Y, Kohshi K, Kunugita N, Tosaki T, Yokota A. Preservation of tumour oxygen after hyperbaric oxygenation monitored by magnetic resonance imaging. *Br J Cancer* 2000; **82**: 88–92. https://doi.org/10.1054/bjoc.1999.0882
68. Matsumoto K, Bernardo M, Subramanian S, Choyke P, Mitchell JB, Krishna MC, et al. Mr assessment of changes of tumor in response to hyperbaric oxygen treatment. *Magn Reson Med* 2006; **56**: 240–46. https://doi.org/10.1002/mrm.20961
69. Baker LCJ, Sikka A, Price JM, Boult JKR, Lepicard EY, Box G, et al. Evaluating imaging biomarkers of acquired resistance to targeted EGFR therapy in xenograft models of human head and neck squamous cell carcinoma. *Front Oncol* 2018; **8**: 271. https://doi.org/10.3389/fonc.2018.00271
70. Zhou H, Habib AA, Mason RP, Zhao D. Integrated MRI approaches to interrogate tumor oxygenation and vascular perfusion of orthotopic brain tumors in a mouse model. Proc Intl Soc Mag Reson Med. 2010;18:2793.